Paradigm
reference-global.com
DOI: 10.2478/agriceng-2026-0003

ISSN 2083-1587; e-ISSN 2449-5999
2026,Vol. 30,No.1, pp. 49-61
Agricultural Engineering
https://agriceng.org

EXPERIMENTAL INVESTIGATION OF SINGLE FLARE IN BRAKE TUBES

Marek Boryga[a*], Bartłomiej Wrzesiński[b]

[a] Department of Mechanical Engineering and Automation, University of Life Sciences in Lublin, Głęboka 28, 20-612 Lublin, Poland,e-mail: marek.boryga@up.lublin.pl, ORCID 0000-0002-5991-7871

[b] S-Machines sp. z o.o. Jana Kilińskiego 86, 22-400 Zamość, Poland, e-mail: bartek.kstaww@gmail.com

Corresponding author: e-mail: marek.boryga@up.lublin.pl

ARTICLE INFO

Article history:
Received: May 2025
Received in the revised form: November 2025
Accepted: December 2025

Keywords:
brake tube,
single flare (SF),
flare diameter,
initial protrusion

ABSTRACT

This study presents the results of experimental tests on single flare (SF) terminations in brake tubes with diameters of ∅4.75 mm and ∅6.35 mm, and wall thickness of 0.9 mm and 1 mm, respectively, using the FALCON toolset. The research aimed at determining the optimal range of initial tube protrusion that results in a flare diameter compliant with the BN-90 3617-09 standard. The paper provides a detailed description of the testing methodology It presents raw measurement data, statistical calculations, and their analysis. Conformity or nonconformity with the specification was assessed according to the guidelines outlined in the PN-EN ISO 14253-1:2018-02 standard. For tubes with the diameter of ∅4.75 mm and the wall thickness of 0.9 mm, the average measured flare diameters for the initial protrusion in the range of 4.4–5.0 mm fall within the tolerance specified by the standard. However, when accounting for measurement uncertainty, the required flare diameters are obtained for the initial protrusion in the range of 4.6–5.0 mm. In the case of tubes with the diameter of ∅6.35 mm and the wall thickness of 1.0 mm, the average measured flare diameters meet the standard requirements for the initial protrusion of 4.6–5.0 mm, whereas, considering the measurement uncertainty, the required flare diameters are obtained for the initial protrusion in the range of 4.8–5.0 mm.

Introduction

The use of passenger cars in agriculture, though often underestimated, plays a crucial role in daily farm operations. These vehicles are utilized not only for transporting workers and light materials but also serve as essential tools for farm management. While this topic remains relatively niche, there are scientific publications addressing the equipment and transportation means used on farms with different types of agricultural production (Kuboń, 2007; Kuboń and Kurzawski, 2013). Road transport safety has been widely discussed in the literature

(Droździel et al., 2014; Ágoston and Madlenák, 2020; Caban et al., 2020; Hudec et al., 2021; Ondruš et al., 2024); however, publications focusing specifically on the safety of vehicles operated under agricultural and off-road conditions remain scarce.

In agriculture, where passenger vehicles frequently operate under challenging terrain and variable operational conditions, the reliability of safety-critical vehicle systems becomes particularly significant. Among these systems, the proper and reliable operation of hydraulic systems – especially braking systems – is of fundamental importance to the safe use of vehicles (Idzikowski and Salamon, 2011; Wilczarska et al., 2018). Therefore, systematic inspections of braking-system performance are essential and are typically conducted using diagnostic methods as part of periodic technical vehicle inspections (Kuliś and Żółtowski, 2011; Hudec et al., 2021a; Hudec and Šarkan, 2022).

Analyses of failures in vehicle safety systems and their consequences indicate that the highest number of malfunctions is associated with braking systems (Droździel et al., 2014; Wojtas and Szkoda, 2018; Rybicka et al., 2018; Jilek and Berg, 2021). In addition, studies addressing accident consequences and vehicle deformation demonstrate that failures of safety-related systems may significantly affect accident severity and vehicle damage (Kubiak et al., 2018). Vehicle tires, which directly influence braking effectiveness, adhesion and vehicle stability, also represent a frequent source of safety-related issues (Caban et al., 2019; Drozd et al., 2022).

The technical quality of working fluids used in vehicle systems has a significant impact on system reliability and operational safety. In particular, the quality and degradation of brake fluid strongly affect the effectiveness of hydraulic braking systems, as confirmed by numerous studies (Caban et al., 2015; Kuranc et al., 2018; Sejkorová et al., 2018; Kopčanová et al., 2020; Caban et al., 2021). Similar degradation mechanisms and their influence on system performance have also been observed for other operating fluids in vehicles and machines used under demanding conditions (Sejkorová and Glos, 2017).

Comparable relationships between operating conditions, system reliability and component wear have been reported for non-standard and special-purpose vehicles, including those used in agriculture, forestry, military applications and recreational activities (Borawski et al., 2020; Przywara et al., 2023). Idzikowski (2011) analyzed the most common malfunctions in hydraulic braking, steering and suspension systems and their impact on braking performance and road safety. Despite the importance of braking systems in such vehicles, only a limited number of publications focus on the modelling and monitoring of hydraulic braking systems. Idzikowski and Salamon (2013) and Idzikowski (2017) proposed mathematical models for diagnosing brake-fluid leakage, incorporating selected braking-system components and enabling more advanced diagnostic approaches. In parallel, machine-learning-based methods for monitoring hydraulic braking systems have been investigated, particularly through the analysis of vibration signals, offering improved fault-detection accuracy (Jegadeeshwaran and Sugumaran, 2013, 2015).

Recent studies emphasize the rapid development of modern braking technologies and their direct impact on road safety (Jilek and Nemec, 2020; Šarkan et al., 2020; Gogola et al., 2022; Szpica et al., 2022; Borawski et al., 2023). Particular attention has been devoted to Anti-lock Braking Systems (ABS), Autonomous Emergency Braking (AEB) and Electronic Stability Control (ESC), which significantly contribute to reduction of accident risk and injury severity (Maia, 2019; Fujiwara and Takechi, 2021; Hu et al., 2023). These technologies

are increasingly implemented not only in passenger cars but also in commercial and specialized vehicles, including those used in agricultural environments.

Furthermore, current research highlights the growing role of simulation and predictive modelling in the analysis and design of brake systems. Innovative approaches, such as fuzzy timed Petri nets (Serji et al., 2023) and integrated control-system simulations based on software environments like MATLAB Simulink (Ann Josy et al., 2025), support the development of more reliable and responsive braking components. In this context, these advances underscore the importance of precision in the design and manufacture of hydraulic braking-system elements, including brake tubes and their connections, which are critical for maintaining hydraulic integrity and system tightness under operational loads (Pliassounov, 2007; BN-90/3617-09).

In modern brake systems, sealing rings, adhesives and washers are not used in tube connections. Sealing must be achieved exclusively through clamping force, ensuring that the connected components can withstand the high hydraulic pressure within the system. A typical connection consists of a port (receiver) with a socket, a flared brake tube and a threaded fitting, which creates a sealed interface between the socket and the tube. The importance of geometric precision in such connections has been highlighted by Pliassounov (2007), who noted that even minor dimensional deviations or assembly disturbances can compromise seal integrity in standardized brake-tubing threaded connectors. Despite this, the literature contains very few quantitative studies linking the initial tube protrusion during forming to the resulting single-flare (SF) diameter and its compliance with BN-90/3617-09 – an operationally important gap that the present study addresses.

Currently, two types of flares are used in the automotive industry. The most common is the single flare (SF). The name derives from the operating cycle of the flaring tool which, in this case, consists of a single-stage operation. Here, the concave socket within the port mates with the convex flare of the brake tube, forming a secure connection. The double flare (DF) is also named based on the operating cycle of the flaring tool, which includes two stages. The first stage forms a single flare (SF), and in the second stage the flare is further shaped into a funnel-like contour. In this configuration, the convex socket inside the port mates with the concave flare of the tube, ensuring a robust connection through the increased contact surface area. The SF offers several advantages over the DF: it requires fewer forming operations, utilizes simpler tooling and allows for easier quality control during manufacture. These factors contribute to its widespread adoption in the automotive industry.

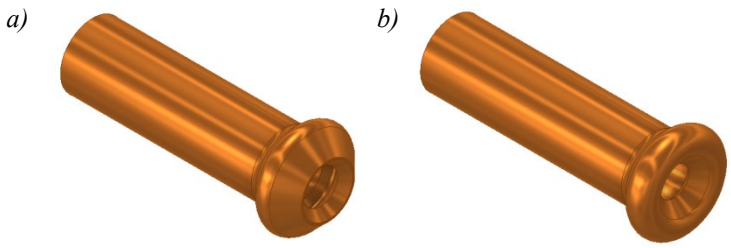

Figure 1. 3D models of brake-tube flares: (a) SF, (b) DF

Great emphasis is placed on the shape and dimensions of the flare during its formation, as these factors ensure that the tube material effectively seals the space between the socket and the threaded fitting. The BN-90/3617-09 standard specifies the exact dimensional requirements for flared hydraulic tubes. Additionally, it allows for alternative materials to the recommended steel, which has the following chemical composition: C ≤ 0.08%, Si ≤ 0.08%, Mn = 0.3–0.45%, P ≤ 0.02%, S ≤ 0.025%, Al = 0.02–0.05%, and the following mechanical properties: Rm ≤ 420 MPa, Re ≤ 300 MPa, $A_5 \geq 25\%$. The tube may also be made from the following materials:

– ZISTA 07 steel tubes,
– seamless precision steel tubes according to PN-73/H-74240,
– low-carbon galvanized steel tubes with a polyamide coating,
– drawn brass tubes (grade M63) in the temper states "r" or "z4" according to PN-77/H-74586/01,
– drawn copper tubes in the grades M1E, M1R, M2G, M2R in a semi-hard state (z4).

The PN-EN 12449:2023-11 standard also defines material properties applicable to brake tubes.

Considering the significance of proper flare geometry for leak-tight connections and compliance with standard requirements, a detailed experimental study was conducted. The aim of this study is to experimentally determine the optimal initial extension length of brake tubes when using a die flaring tool, in order to meet the geometrical requirements specified in BN-90/3617-09. This study quantifies the relationship between the initial protrusion of the brake tube beyond the die face and the resulting single-flare diameter d_2 for two tube sizes, computes the associated measurement uncertainty, and identifies protrusion ranges that ensure compliance with BN-90/3617-09 when using a Falcon-type die flaring tool.

Materials and Methods

The study investigated single-flare (SF) formations on brake tubes of two nominal diameters – ∅4.75 mm (wall 0.9 mm) and ∅6.35 mm (wall 1.0 mm) – produced using a Falcon-type die flaring tool. The subsequent subsections describe specimen preparation, the trial series to bound the feasible protrusion l, the measurement series (l = 4.0–5.0 mm in 0.2 mm steps), the metrological procedure, and the statistical/uncertainty treatment used for conformity assessment against BN-90/3617-09.

The subject of this research was single flares (SF) formed on brake tubes with outer diameters of 4.75 mm and 6.35 mm and wall thicknesses of 0.9 mm and 1 mm, respectively. The flares were formed using a Falcon flaring tool set. The experimental procedure consisted of the following steps:

– preparation of samples,
– conducting preliminary flaring trials to determine the feasible range of initial extensions,
– performing test flaring operations,
– measuring flare diameters and conducting statistical analysis,
– drawing conclusions.

Sample preparation involved cutting copper brake tubes to a length of 24 mm, regardless of tube size. The cuts were made using a specialized cutter designed for rigid copper tubing, followed by deburring to eliminate any sharp edges or material residues. The selected length

facilitated proper positioning within the flaring device and ensured consistent shaping (Wrzesiński, 2020).

The Falcon kit includes a manual flaring press and a set of forming dies. In each case, the copper tube segment was clamped in the split die, and its end was extended beyond the die face (initial protrusion). Before performing the main test series, preliminary flares were made to identify the acceptable range of protrusion. It was observed that protrusions above 5.0 mm caused excessive material deformation or buckling, while values below 4.0 mm resulted in underformed flares. Based on these observations, the test range of initial extensions was set between 4.0 mm and 5.0 mm, at 0.2 mm intervals.

Figure 2 illustrates the reference shape and dimensions of a properly formed single flare (SF) as specified in the BN-90/3617-09 standard.

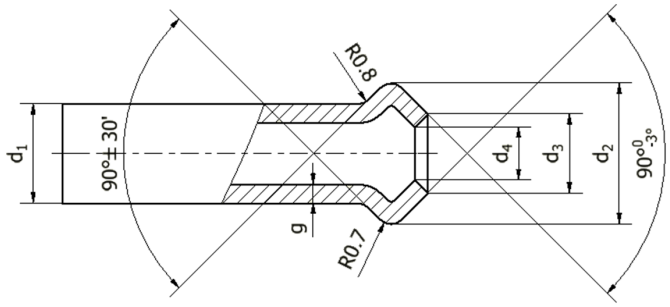

Figure 2. Dimensions of single flare (SF) according to the BN-90/3617-09 standard

After completing the flaring process, the external diameters d_2 of the copper brake tube ends were measured at four equidistant positions spaced 45° apart around the flare circumference. Measurements were performed using a Mitutoyo micrometer with a measuring range of 0–25 mm and the maximum permissible error (*MPE*) of 0.01 mm (Wrzesiński, 2020). To evaluate the measurement uncertainty, both Type A (based on statistical analysis of repeated measurements) and Type B (based on instrument specifications) standard uncertainties were taken into account. The Type A standard uncertainty (standard deviation of the mean) was calculated using the formula:

$$u_A(d) = \frac{\sigma_d}{\sqrt{N}} = \sqrt{\frac{\sum_{n=1}^{N}(d_i - \overline{d})^2}{N(N-1)}} \tag{1}$$

where:

σ_d – standard deviation of the flare diameter,
N – number of measurements,
d_i – individual flare diameter measurements,
$\overline{d}$ – mean flare diameter.

The Type B standard uncertainty, related to the micrometer's accuracy, was calculated as:

$$u_B(d) = \frac{MPE}{\sqrt{3}} \tag{2}$$

where:
MPE – maximum permissible error of the measuring instrument.

The combined standard uncertainty was determined by:

$$u_C(d) = \sqrt{u_A^2(d) + u_B^2(d)} \tag{3}$$

Finally, the expanded uncertainty was estimated using:

$$U(d) = k \cdot u_C(d) \tag{4}$$

where:
k – expansion coefficient.

Given the small sample size (N=4), the expansion factor k=3.18 was selected from the Student's t-distribution for 3 degrees of freedom and a confidence level of 95%.

Results and Discussion

The results of the flare diameter d_2 measurements for the tubes with the diameter of ∅4.75 mm and the wall thickness of 0.9 mm are presented in Table 1, while those for the tubes with the diameter of ∅6.35 mm and the wall thickness of 1 mm are summarized in Table 2.

Table 1.
Results of measurements and calculations for the tube with the diameter of ∅4.75 mm and the wall thickness of 0.9 mm

Quantity	Designation	Initial protrusion l (mm)					
		4.0	4.2	4.4	4.6	4.8	5.0
Diameter after flaring*	d_2 (mm)	6.5	6.59	6.65	6.73	6.88	6.77
		6.47	6.57	6.67	6.74	6.83	6.76
		6.54	6.59	6.68	6.72	6.84	6.74
		6.53	6.54	6.55	6.68	6.83	6.83
Arithmetic mean	$\bar{d}_2$ (mm)	6.510	6.573	6.638	6.718	6.845	6.775
Type A uncertainty	$u_A(d_2)$ (mm)	0.016	0.012	0.030	0.013	0.012	0.019
Type B uncertainty	$u_B(d_2)$ (mm)	0.012					
Total uncertainty	$u_C(d_2)$ (mm)	0.020	0.017	0.032	0.018	0.017	0.023
Expansion coefficient	k	3.18					
Expanded uncertainty	$U(d_2)$ (mm)	0.062	0.053	0.102	0.056	0.053	0.072

* - based on (Wrzesiński, 2020).

Table 2.
Results of measurements and calculations for the tube with the diameter of ∅6.35 mm and the wall thickness of 1 mm

Quantity	Designation	Initial protrusion l (mm)					
		4.0	4.2	4.4	4.6	4.8	5.0
Diameter after flaring*	d_2	8.44 8.43 8.42 8.43	8.24 8.26 8.27 8.23	8.42 8.41 8.43 8.45	8.73 8.80 8.79 8.67	8.81 8.90 8.88 8.83	8.92 8.94 8.95 8.93
Arithmetic mean	$\bar{d}_2$ (mm)	8.430	8.250	8.428	8.746	8.855	8.935
Type A uncertainty	$u_A(d_2)$ (mm)	0.004	0.009	0.009	0.030	0.021	0.006
Type B uncertainty	$u_B(d_2)$ (mm)	0.012					
Total uncertainty	$u(d_2)$ (mm)	0.012	0.015	0.014	0.032	0.024	0.013
Expansion coefficient	k	3.18					
Expanded uncertainty	$U(d_2)$ (mm)	0.039	0.047	0.046	0.103	0.076	0.042

* based on (Wrzesiński, 2020).

In Table 3 the measurement results of the flare diameter d_2, along with the uncertainty, for the tubes with the diameters of ∅4.75 mm and ∅6.35 mm are presented.

Table 3.
Summary of the diameters d_2 obtained from the flares for the tubes with the diameters of ∅4.75 mm and ∅6.35 mm for the applied initial protrusion l.

Initial protrusion l (mm)	Measurement result of the flare diameter d_2 (mm)	
	Diameter 4.75 mm	Diameter 6.35 mm
4.0	6.51 ± 0.06	8.43 ± 0.04
4.2	6.57 ± 0.05	8.25 ± 0.05
4.4	6.64 ± 0.10	8.43 ± 0.05
4.6	6.72 ± 0.06	8.75 ± 0.10
4.8	6.85 ± 0.05	8.86 ± 0.08
5.0	6.78 ± 0.07	8.94 ± 0.04

In Figure 3 the scatter plot of the flare diameter d_2 of the tube with the diameter of 4.75 mm is presented as a function of the initial protrusion l, along with the determined uncertainty and the specified limit dimensions defined by the BN-90/3617-09 standard.

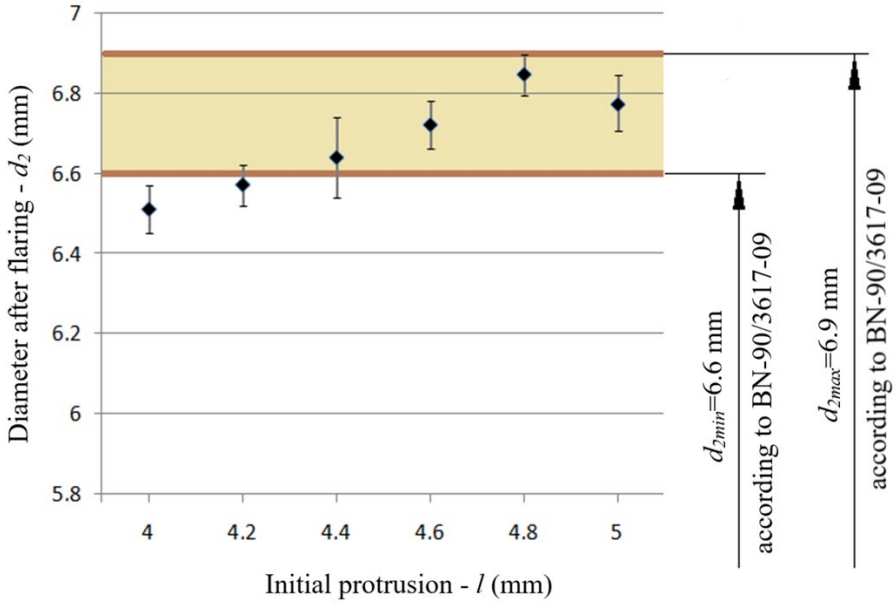

Figure 3. Observed values of the flare diameter as a function of the initial protrusion for the tube with a diameter of ∅4.75 mm, showing the uncertainty and the specified limit dimensions defined by the BN-90/3617-09 standard

The average measurement values for the initial protrusion l ranging from 4.4 to 5.0 mm fall within the tolerance ranges specified in the BN-90/3617-09 standard. However, considering the measurement uncertainty, the required flare diameters d_2 will be obtained for the initial protrusion in the range of 4.6 to 5.0 mm.

Figure 4 presents the scatter plot of the flare diameter d_2 of the tube with a diameter of 6.35 mm.

In this case the average measurement values for the initial protrusion l ranging from 4.6 to 5.0 mm fall within the tolerance ranges specified in the BN-90/3617-09 standard. Considering the measurement uncertainties, the required flare diameters d_2 will be obtained for the initial protrusion in the range of 4.8 to 5.0 mm. The results clearly show that insufficient or excessive initial protrusion leads to deviations in the flare diameter, which may affect the conformity with the BN-90/3617-09 standard. In particular, excessive protrusion resulted in oversized flares, while shorter protrusion often produced undersized or asymmetrical flares. These findings are consistent with the observations made by Pliassounov (2007), who emphasized that even minor geometric inaccuracies or assembly-related disturbances in brake tube connections can significantly compromise sealing performance. The flare geometry, especially in single flare systems where no sealing rings are used, plays a crucial role in achieving leak-free connections. Therefore, the observed sensitivity of flare diameter to protrusion length confirms the importance of strictly controlling this parameter during tube forming.

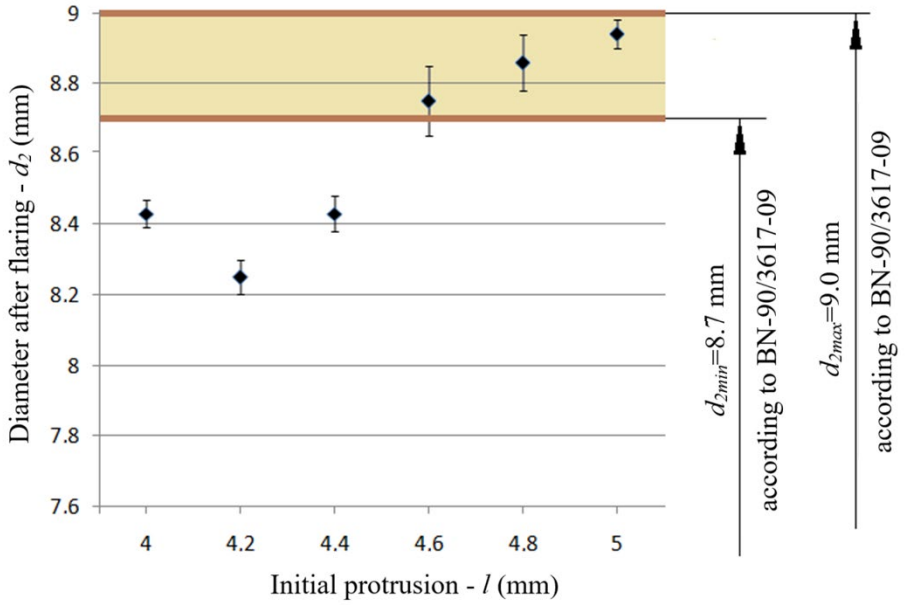

Figure 4. Observed values of the flare diameter as a function of the initial protrusion for the tube with the diameter of ∅6.35 mm, with indicated uncertainty and marked limit dimensions specified by the BN-90/3617-09 standard

Conclusions

Based on the results presented in this study the following conclusions can be drawn:

1. For the tube with a diameter of ∅4.75 mm and wall thickness of 0.9 mm, the average measurement values for the initial protrusions in the range of 4.4 to 5.0 mm fall within the tolerance ranges specified in the BN-90/3617-09 standard. Additionally, considering the measurement uncertainty, the required flared diameters will be obtained for the initial protrusion in the range of 4.6 to 5.0 mm.
2. For the tube with a diameter of ∅6.35 mm and wall thickness of 1.0 mm, the average measurement values for the initial protrusions in the range of 4.6 to 5.0 mm fall also within the tolerance ranges specified in the BN-90/3617-09 standard. Moreover, considering the measurement uncertainties, the required flared diameters will be obtained for the initial protrusion in the range of 4.8 to 5.0 mm.

The results of the experimental studies were utilized in the design of a hydraulic press for flaring tubes. Pairs of dies with dimensions ensuring the appropriate initial protrusion were applied (Wrzesiński, 2020).

Author Contributions: Conceptualization, M.B. and B.W.; methodology, M.B. and B.W.; software, M.B.; validation, M.B.; formal analysis, M.B.; investigation, B.W.; resources, B.W.; data curation, B.W.; writing – original draft preparation, M.B.; writing-review and editing, M.B.; visualization, M.B. and B.W.; supervision, M.B.; project administration, M.B. All authors have read and agreed to the published version of the manuscript.

Conflicts of Interest: The authors declare no conflict of interest.

Funding: This research received no external funding.

References

Ann Josy, T., Sadique, A., Thomas, M., Manaf T. M. A. & Vr, S. (2025). Software Architecture for Autonomous Vehicles using MATLAB Simulink. *SAE Technical Paper*, 2025-28-0190. 2025. https://doi.org/10.4271/2025-28-0190.

Ágoston, G., & Madlenák, R. (2020). Road safety macro assessment model: Case study for Hungary. *Periodica Polytechnica Transportation Engineering*, *49*(1), 89-92. https://doi.org/10.3311/PPtr.13083.

Borawski, A., Mieczkowski, G., & Szpica, D. (2020). Simulation tests of peripheral friction brake used in agricultural machinery shafts. *Engineering for Rural Development*, *19*, 494-502. https://doi.org/10.22616/ERDev.2020.19.TF112.

Borawski, A., Mieczkowski, G., & Szpica, D. (2023). Composites in Vehicles Brake Systems-Selected Issues and Areas of Development. *Materials*, *16*(6), 2264. https://doi.org/10.3390/ma16062264.

Caban, J., Marczuk, A., Šarkan, B., & Vrábel, J. (2015). Studies on operational wear of glycol-based brake fluid. *Przemysl Chemiczny*, *94*(10), 1802-1806. https://doi.org/10.15199/62.2015.10.30.

Caban, J., Turski, A., Nieoczym, A., Tarkowski, S., & Jereb, B. (2019). Impact of specific factors on the state of the tire pressure value. Archives of Automotive Engineering, 85(3), 137-148. https://doi.org/10.14669/AM.VOL85.ART10.

Caban, J., Drozdziel, P., Stoma, M., Dudziak, A., Vrabel, J., & Stopka, O. (2020). Road Traffic Safety in Poland, Slovakia and Czech Republic-Statistic Analysis. *12th International Science-Technical Conference Automotive Safety 2020, 21-23 October 2020, Kielce, Poland*, 9293507. ISBN:978-1-7281-5813-6.

Caban, J., Vrábel, J., Šarkan, B., Kuranc, A., & Słowik, T. (2021). Operational tests of brake fluid in passenger cars. *Periodica Polytechnica Transportation Engineering*, *49*(2), 126-131. https://doi.org/10.3311/PPtr.14583.

Drozd, K., Tarkowski, S., Caban, J., Nieoczym, A., Vrábel, J., & Krzysiak, Z. (2022). Analysis of Truck Tractor Tire Damage in the Context of the Study of Road Accident Causes. *Applied Sciences*, *12*(23), 12333. https://doi.org/10.3390/app122312333.

Droździel, P., Krzywonos, L., Madlenak, R., & Rybicka, I. (2014). Selected aspects of analyses of failure rates of active safety systems in buses. *Communications - Scientific Letters of the University of Žilina*, *16*(3), 114-119. https://doi.org/10.26552/com.C.2014.3.114-119.

Fujiwara, T. & Takechi, K. (2021). Making the world safer: Autonomous emergency braking systems enhance safety for senior drivers. *Applied Economics Letters*, *29*(13), 1177–1181. https://doi.org/10.1080/13504851.2021.1917760.

Gogola, M., Ondruš, J., Kubalak, S., & Turiak, P. (2022). Comparison of braking properties of selected vehicle with different methods. *Archives of Automotive Engineering*, *95*, 1, 5-17. https://doi.org/10.14669/AM.VOL95.ART1.

Hu, L., Li, H., Yi, P., Huang, J., Lin, M. & Wang, H. (2023). Investigation on AEB Key Parameters for Improving Car to Two-Wheeler Collision Safety Using In-Depth Traffic Accident Data, *IEEE Transactions on Vehicular Technology*, *72*(1), 113-124. https://doi.org/10.1109/TVT.2022.3199969.

Hudec, J., Šarkan, B., Caban, J., & Stopka, O. (2021). The impact of driving schools' training on fatal traffic accidents in the Slovak Republic. *Scientific Journal of Silesian University of Technology. Series Transport*, *110*, 45-57. https://doi.org/10.20858/sjsutst.2021.110.4.

Hudec, J., Šarkan, B., & Czodörová, R. (2021a). Examination of the results of the vehicles technical inspections in relation to the average age of vehicles in selected EU states. *Transportation Research Procedia*, *55*, 2-9. https://doi.org/10.1016/j.trpro.2021.07.063.

Hudec, J., & Šarkan, B. (2022). Effect of periodic technical inspections of vehicles on traffic accidents in the Slovak Republic. *Communications - Scientific Letters of the University of Žilina*, *24*(3), A142-A159. https://doi.org/10.26552/com.C.2022.3.A142-A159.

Idzikowski, A. (2011). Stan techniczny i wyposażenie pojazdów samochodowych a bezpieczeństwo ruchu drogowego. *Polskie Stowarzyszenie Zarządzania Wiedzą: Studia i Materiały*, *46*, 94-106.

Idzikowski, A. (2017). Boolean model of HSUH leakage testing for the purpose of designing a diagnosing unit of selected damages of vehicle braking mechanisms. *The Archives of Automotive Engineering - Archiwum Motoryzacji*, *78*(4), 79-92. https://doi.org/10.14669/AM.VOL78.ART6.

Idzikowski, A., & Salamon, S. (2011). Jakość konstrukcyjna elementów układu hamulcowego a bezpieczeństwo ruchu drogowego. *Polskie Stowarzyszenie Zarządzania Wiedzą: Studia i Materiały*, *47*, 92-108.

Idzikowski, A., & Salamon, S. (2013). Mathematical model for the diagnostics of vehicle hydraulic braking system leakage. *The Archives of Automotive Engineering - Archiwum Motoryzacji*, *61*(3), 13-23.

Jegadeeshwaran, R., & Sugumaran, V. (2013). Comparative study of decision tree classifier and best first tree classifier for fault diagnosis of automobile hydraulic brake system using statistical features. *Measurement*, *46*, 3247–3260. https://doi.org/10.1016/j.measurement. 2013.04.068.

Jegadeeshwaran, R., & Sugumaran, V. (2015). Fault diagnosis of automobile hydraulic brake system using statistical features and support vector machines. *Mechanical Systems and Signal Processing*, *52-53*, 436–446. https://doi.org/10.1016/j.ymssp.2014.08.007.

Jilek, P., & Berg, J. (2021). Optimization of device allowing variation of adhesion force for road vehicle testing at safe speed. *Engineering for Rural Development*, *20*, 373-378. https://doi.org/10.22616/ERDev.2021.20.TF078.

Jilek, P., & Nemec, J. (2020). Changing adhesion force for testing road vehicles at safe speed. *Engineering for Rural Development*, *19*, 1411-1417. https://doi.org/10.22616/ERDev.2020. 19.TF351.

Kopčanová, S., Sejkorová, M., Kučera, M., & Hnilicová, M. (2020). Wear of hydraulic system components assessment based on the analysis of hydraulic oil degradation degree. *Przemysl Chemiczny*, *99*(9), 1399-1403. https://doi.org/10.15199/62.2020.9.XX.

Kubiak, P., Krzemieniewski, A., Lisiecki, K., Senko, J., & Szosland, A. (2018). Precise method of vehicle velocity determination basing on measurements of car body deformation–non-linear method for 'Full Size' vehicle class. International Journal of Crashworthiness, *23*(3), 302-310. https://doi.org/10.1080/13588265.2017.1331692.

Kuboń, M. (2007). Wyposażenie i wykorzystanie środków transportowych w gospodarstwach o różnym typie produkcji rolniczej. *Inżynieria Rolnicza*, *8*(96), 141-148.

Kuboń, M., & Kurzawski D. (2013). Kierunek produkcji a wyposażenie i wykorzystanie środków transportowych w wybranych gospodarstwach rolnych. *Inżynieria Rolnicza*, *2*(143), 191-200.

Kuliś, E., & Żółtowski, B. (2011). Badania układów hamulcowych. *Polskie Stowarzyszenie Zarządzania Wiedzą: Studia i Materiały*, 47, 126-140. ISSN 1732-324X.

Kuranc, A., Zając, G., Szyszlak-Bargłowicz, J., Słowik, T., Vrăbel, J., Šarkan, B., Caban, J., & Makarski, P. (2018). Boiling point of the brake fluid based on alkyl ethers of alkylene glycols in vehicles being in use. *Przemysl Chemiczny*, *97*(12), 2102-2105. https://doi.org/10.15199/62.2018.12.17.

Maia, I. D. de C. D. (2019). Modeling and control of anti-lock braking systems considering different representations for tire–road interaction. In *23rd International Conference on System Theory, Control and Computing* pp. 344-349. https://doi.org/10.1109/ICSTCC.2019.8885694.

Ondruš, J., Jančár, A., Gogola, M., Varga, P., Šarić, Ž., & Caban, J. (2024). Smartphone Sensors in Motion: Advancing Traffic Safety with Mobile Technology. *Applied Sciences*, *14*(13), 5404. https://doi.org/10.3390/app14135404.

Pliassounov, S. (2007). Fundamentals and common problems of seal integrity robustness of standardized brake tubing threaded connectors. *SAE Technical Paper*, 2007-01-0557. https://doi.org/10.4271/2007-01-0557.

Przywara, A., Kraszkiewicz, A., Koszel, M., Atanasov, A.Z., & Parafiniuk, S. (2023). The Structure of Engine Power of Agricultural Tractors Registered in Poland Between 2010 and 2020. *Lecture Notes in Civil Engineering*, 289, 1-14. https://doi.org/10.1007/978-3-031-13090-8_1.

Rybicka, I., Caban, J., Vrábel, J., Šarkan, B., Stopka, O., & Misztal, W. (2018). Analysis of the safety systems damage on the example of a suburban transport enterprise. 11th International Science and Technical Conference Automotive Safety, AUTOMOTIVE SAFETY 2018, 18-20 April 2018, Casta, Papiernicka, Slovakia, pp. 1–6. https://org.doi/10.1109/ AUTOSAFE.2018.8373323.

Sejkorová, M., & Glos, J. (2017), Analysis of degradation of motor oils used in zetor tractors. Acta Universitatis Agriculturae et Silviculturae Mendelianae Brunensis, *65*(1), 179-187. https://doi.org/10.11118/actaun201765010179.

Sejkorová, M., Verner, J., Sejkora, F., Hurtová, I., & Senkýř, J. (2018). Analysis of operation wear of brake fluid used in a Volvo car. *Transport Means - Proceedings of the International Conference*, 2018, 3-5 October 2018, Trakai, pp. 592-596.

Serji, A., Mermri, E. B., & Blej, M. (2023). Modeling Automatic Emergency Braking System Using Fuzzy Timed Petri Nets Based on the 3-Second Rule, *2023 International Conference on Electrical, Computer and Energy Technologies*, Cape Town, South Africa, 1-6, https://doi.org/10.1109/ICECET58911.2023.10389413.

Szpica, D., Kisiel, M., & Czaban, J. (2022). Simulation Evaluation of the Influence of Selected Geometric Parameters on the Operation of the Pneumatic Braking System of a Trailer with a Differential Valve. *Acta Mechanica et Automatica*, *16*(3), 233-241. https://doi.org/ 10.2478/ama-2022-0028.

Šarkan, B., Jaśkiewicz, M., & Kiktová, M. (2020). The impact of the truck loads on the braking efficiency assessment. Open Engineering, *10*(1), 105-112. https://doi.org/10.1515/eng-2020-0014.

Wilczarska, J., Kuliś, E., & Matuszewski, M. (2018). Characteristics of hydraulic systems used in vehicles other than machines at work. *Autobusy: technika, eksploatacja, systemy transportowe*, *12,* 2018, 701-705. https://doi.org/10.24136/atest.2018.482.

Wojtas, A., & Szkoda, M. (2018). Analiza wybranych czynników wpływających na bezpieczeństwo w ruchu drogowym. *Autobusy: technika, eksploatacja, systemy transportowe*, *19*(6), 1149-1154. https://doi.org/10.24136/atest.2018.244.

Wrzesiński, B. (2020). Badania spęczeń przewodów hamulcowych dla modelu hydraulicznej zakuwarki. *Praca magisterska, Uniwersytet Przyrodniczy w Lublinie*.

BN-90/3617-09. Hydrauliczne układy hamulcowe. Przewody metalowe.

PN-EN 12449:2023-11. Miedź i stopy miedzi -- Rury okrągłe bez szwu ogólnego przeznaczenia.

PN-EN ISO 14253-1:2018-02. Specyfikacje geometrii wyrobów (GPS) -- Kontrola wyrobów i wyposażenia pomiarowego za pomocą pomiarów -- Część 1: Reguły orzekania zgodności lub niezgodności ze specyfikacją.

BADANIA EKSPERYMENTALNE POJEDYNCZEGO ROZSZERZENIA PRZEWODÓW HAMULCOWYCH

Streszczenie. W niniejszym opracowaniu przedstawiono wyniki badań eksperymentalnych zakończeń pojedynczego rozszerzenia (SF) przewodów hamulcowych o średnicach ∅4,75 mm i ∅6,35 mm oraz grubościach ścianek odpowiednio 0,9 mm i 1 mm, z wykorzystaniem zestawu narzędzi FALCON. Celem badań było określenie optymalnego zakresu początkowego wysunięcia przewodu, który skutkuje średnicą rozszerzenia zgodną z normą BN-90 3617-09. W artykule przedstawiono szczegółowy opis metodyki badań, przedstawiono surowe dane pomiarowe, obliczenia statystyczne i ich analizę. Zgodność lub niezgodność ze specyfikacją oceniono zgodnie z wytycznymi określonymi w normie PN-EN ISO 14253-1:2018-02. Dla przewodów o średnicy ∅4,75 mm i grubości ścianki 0,9 mm, średnie zmierzone średnice rozszerzenia dla początkowego wysunięcia w zakresie 4,4–5,0 mm mieszczą się w tolerancji określonej normą. Jednakże, uwzględniając niepewność pomiaru, wymagane średnice rozszerzenia uzyskuje się dla początkowego wysunięcia w zakresie 4,6–5,0 mm. W przypadku przewodów o średnicy ∅6,35 mm i grubości ścianki 1,0 mm, średnie zmierzone średnice rozszerzenia spełniają wymagania normy dla początkowego wysunięcia 4,6–5,0 mm. Natomiast, uwzględniając niepewność pomiaru, wymagane średnice rozszerzenia uzyskuje się dla początkowego wysunięcia w zakresie 4,8–5,0 mm.

Słowa kluczowe: przewód hamulcowy, pojedyncze rozszerzenie (SF), średnica rozszerzenia, początkowe wysunięcie